

Utilization of spent coffee grounds as fillers to prepare polypropylene composites for food packaging applications

Yurong Cai¹, Wenmin Song¹, Yuncong Yang¹, Xiuwen Cheng¹, Mingming Jiang¹, Ruizhang², and Jiri Militky³

¹Zhejiang Sci-Tech University

²NMG Composites CoLtd

³Faculty of Textile, Technical University of Liberec, 46117 Liberec, Czech Republic

February 10, 2023

Abstract

Biomass-derived wastes as the additive of non-degradable plastics have been paid more attention due to the ever-growing environmental pollution and energy crisis. Herein, the spent coffee grounds (SCG) have been used as fillers in polypropylene (PP) after the heat treatment to realize its recycling utilization. The effect of the heat treatment atmosphere on the properties of the obtained SCG and SCG/PP composites has been investigated systematically. The results show that the residual coffee oil can be removed more thoroughly under an air atmosphere than under a nitrogen atmosphere at a relatively low cost and an eco-friendly process. The lower residual oil rate of SCG is beneficial to improve the comminution and further enhance the affinity with the PP matrix. The obtained SCG/PP composite holds lower water absorption, higher hydrophobicity, and better mechanical properties, implying its potential applications in the field of food packaging.

Utilization of spent coffee grounds as fillers to prepare polypropylene composites for food packaging applications

Wenmin Song¹, Yuncong Yang¹, Xiuwen Cheng¹, Mingming Jiang¹, Ruizhang², Jiri Militky³, Yurong Cai^{1,*}.

1. The Key Laboratory of Advanced Textile Materials and Manufacturing Technology of Ministry of Education, National Engineering Lab for Textile Fiber Materials and Processing Technology, School of Materials Science and Engineering, Zhejiang Sci-Tech University, Hangzhou 310018, P R China

2. NMG Composites Co.Ltd., Chongfu, Tongxiang, Zhejiang, 314511, China

3. Faculty of Textile, Technical University of Liberec, 46117 Liberec, Czech Republic

*E-mail address:Caiyr@zstu.edu.cn (Cai Y);

Abstract

Biomass-derived wastes as the additive of non-degradable plastics have been paid more attention due to the ever-growing environmental pollution and energy crisis. Herein, the spent coffee grounds (SCG) have been used as fillers in polypropylene (PP) after the heat treatment to realize its recycling utilization. The effect of the heat treatment atmosphere on the properties of the obtained SCG and SCG/PP composites has been investigated systematically. The results show that the residual coffee oil can be removed more thoroughly under an air atmosphere than under a nitrogen atmosphere at a relatively low cost and an eco-friendly process. The lower residual oil rate of SCG is beneficial to improve the comminution and further enhance the affinity with the PP matrix. The obtained SCG/PP composite holds lower water absorption, higher

hydrophobicity, and better mechanical properties, implying its potential applications in the field of food packaging.

Keywords

Spent coffee grounds; heat treatment atmosphere; residual oil rate; composites; mechanical properties

Research highlights

- Spent coffee grounds have been used as fillers in PP after the heat treatment.
- The heat treatment in the air is more favorable for the removal of the coffee oil of SCG.
- The low residual oil rate in SCG can improve its comminution and affinity with PP.
- The SCG/PP composite holds excellent performances for food packaging applications.

1 INTRODUCTION

With the increasing awareness of green environmental protection, the non-incineration utilization of biological waste is one of the subjects that has been widely studied in many countries. Coffee is one of the world's top three drinks, with huge consumption every year (Franca and Oliveira, 2019). Spent coffee grounds (SCG), wastes from the coffee production process, are rich in fiber, oil, and protein (Ballesteros et al., 2014; Bomfim et al., 2022; McNutt and He, 2019) and have been developed to recycle utilization in clothing (Kalebek, 2021), organic fertilizer (Ragauskaitė and Šlinkšienė, 2022; Santhanarajan et al., 2021), medicine (Jamari et al., 2021; Nurman et al., 2021) and other fields. In addition, SCG is contained in natural pigments to dodge or reduce the use of artificial colors (Arya et al., 2022; Koh and Hong, 2019; Parra-Campos and Eduardo Ordonez-Santos, 2019). Biomass natural fiber has the advantages of low cost, abundant sources, and better biodegradability (Madyaratri et al., 2022).

It is worth noting that microplastic (Frias and Nash, 2019) produced by the slight degradation of conventional plastic polypropylene (PP) can directly harm human beings by polluting soil (Watteau et al., 2018; Zhang et al., 2018), fresh water (Rodrigues et al., 2018), and air (Zhang et al., 2020). Degradable plastics are conducive to solving these problems, such as starch-based plastics, polylactic acid (PLA), etc. But their application is always constrained due to the high development costs, certain performance limitations, and immature manufacturing technology.

A certain amount of biodegradable biomass waste is added to traditional plastics as fillers to prepare biomass-plastic composite materials (Bensalah et al., 2021; Qasim et al., 2020), which can effectively utilize the waste biomass resources, reduce the use of plastics and upgrade the degradability of the plastic. The characteristics of SCG, particularly the residual oil content, are vital for the performance of the subsequent SCG/PP composite plastics (Kalebek, 2021). The lower oil content in SCG is believed to obtain composites with a denser fiber structure and higher mechanical properties (Wu et al., 2016; Zarrinbakhsh et al., 2016). The extraction methods of oil from biomass include organic solvent extraction (Mueanmas et al., 2019; Unugul et al., 2020), ultrasonic-assisted extraction (Le et al., 2020), pressurized liquid extraction (de Almeida-Couto et al., 2022) and pyrolysis (Kumar et al., 2020). Hesham Moustafa et al. (Moustafa et al., 2017) heat-treated SCG at 270 °C in the nitrogen atmosphere. The obtained SCG was less oil and more hydrophobic. The resulting SCG/PBAT composite had better mechanical properties. Carmen Branca et al. (Branca et al., 2006, 2005) specified that the non-inert atmosphere is also beneficial to the extraction of bio-oil from cellulose and wood. Nonetheless, the effect of the atmosphere on SCG and SCG plastic composites has not been studied systematically.

In the present study, the effect of heat treatment parameters on the properties of SCG and SCG/PP composite plastics is investigated from the point view of the atmosphere. The results show that the SCG treated under air atmosphere is less oil and higher abrasive than under nitrogen atmosphere at the same temperature, which holds better affinity with PP by increasing the hydrophobicity at a relatively low cost and an eco-friendly process. The resulting SCG/PP composite is lower water absorption, elevated hydrophobicity, and mechanical properties, which have potential applications in the field of food packaging.

2 MATERIALS AND METHODS

2.1 Materials

The Polypropylene T30S (Homopolymer, the density is $0.905 \text{ g}\cdot\text{cm}^{-3}$, the MFI index is $2.6 \text{ g}\cdot 10\text{min}^{-1}$, and the melting point is 170 degC) was purchased from China Petroleum and Chemical Corporation Limited. SCG was from a local coffee shop. Petroleum ether having a boiling range of $60\text{-}90$ with analytical pure was purchased from Hangzhou Gaojing Fine Chemical Co., LTD.

2.2 Preparation of the SCG

The SCG was dried in a 105 degC oven for 24 h, and then the dried SCG was heat treated in a tube furnace under nitrogen and air atmosphere at 240 degC for 1.5 h with the heating speed of $5 \text{ degC}\cdot\text{min}^{-1}$, respectively. The obtained SCG were named as NSCG and ASCG corresponding to the heat treatment atmosphere of nitrogen and air separately.

2.3 Preparation of the composite specimens

The 25 wt.% SCG, NSCG, and ASCG were mechanically mixed with PP, respectively. Then they were processed at $190 \text{ } 60 \text{ rpm}$ for 15 minutes in a torque rheometer with a reverse rotating head. Finally, the obtained samples were pressed into thin sheets at 190 degC for 5 minutes with a pressure of 10 MPa, and then taken out for use after cooling.

2.4 Characterization

2.4.1 Characterization of SCG

Mobile phone camera (Vivo S7), Scanning electron microscope (Vltra 55), and optical microscope (Nikon eclipse ts100) were used to observe the morphologies of SCG. Fourier transform infrared spectrometer was used to analyze the functional groups of SCG before and after heat treatment. Three kinds of SCG powder samples were ground with KBr at a mass ratio of 1:100 and pressed into thin discs. KBr was used as a carrier, and the spectral range is between 4000 and 500 cm^{-1} with 32 scans. The Water contact angle of SCG was measured by a video contact angle instrument (JY-82A). The residual oil content of SCG, NSCG, and ASCG was determined by using a Soxhlet extraction device and petroleum ether was selected as the solvent. If the refractive index of the petroleum ether after extraction is the same as that of the original petroleum ether, it indicates that the oil extraction is complete. The calculation formula of residual oil content is as follows:

$$\omega = \frac{m_{\text{SCG}} - m_{\text{Oil}}}{m_{\text{SCG}}} \times 100\% \quad (1)$$

where m_{SCG} is the mass of SCG and m_{Oil} is the mass of residual oil.

The calculation formula of relative weight loss of NSCG and ASCG is as follows:

$$M = \frac{m_1 - m_2}{m_1} \times 100\% \quad (2)$$

where m_1 is the mass of SCG before heat treatment and m_2 is the mass of SCG after heat treatment.

2.4.2 Characterization of SCG/PP composites

The morphologies of SCG/PP composites was observed by optical microscope (Nikon eclipse ts100). The water contact angle was tested with a video contact angle meter (JY-82A). The samples were dried at 50 for 24 h according to GB-T 1034-2008 to test the water absorption rate. The weight of the dried sample (m_0) was measured with an analytical balance with a precision of 0.01 g . The samples were immersed in tap water at room temperature for 24 h and then removed to measure their weight. The calculation formula of water absorption rate is: water absorption rate = $(m_t - m_0) / m_0 \times 100\%$, where m_0 represents the initial weight and m_t represents the weight of the sample after soaking for 24 h. All tests were performed at room temperature. A thermogravimetric analyzer (NETZSCH TG 209 F1) was used to analyze the thermal decomposition process of samples. The temperature was increased from 30 degC to 600 degC at a rate of $20 \text{ } \cdot \text{min}^{-1}$ under

the nitrogen atmosphere. Thermal analysis of PP, SCG/PP, NSCG/PP, and ASCG/PP composites was performed using differential scanning calorimetry (DSC 25, TA Instruments instrument) equipped with a liquid nitrogen cooling system (REFRIGERATED COOLING SYSTEM 90). 3-8 mg samples were taken respectively. First, the samples were heated from room temperature to 200 degC at a rate of 10 degC*min⁻¹ for 5 minutes, then cooled to room temperature at a cooling rate of 10 degC*min⁻¹, and then heated to 200 degC at the same rate of 10 degC*min⁻¹ for 5 minutes. The minimum nitrogen flow is 50 mL*min⁻¹. The melting enthalpy was obtained during the second heating process and crystallization parameters were obtained through the cooling stage. Crystallinity $X_c = (\Delta H_f / \Delta H_0) \times 100\%$, where ΔH_f is the enthalpy of melting and ΔH_0 is the enthalpy of melting of crystalline PP with crystals of 100% ($\Delta H_0 = 209 \text{ J}\cdot\text{g}^{-1}$). Undercooling degree $\Delta T = T_m - T_c$, where T_m is the equilibrium melting point and T_c is the crystallization temperature. The mechanical properties of the dumbbell-shaped samples were tested by a universal testing machine (INSTRON 5934) at a rate of 50 mm·min⁻¹ according to ASTM D882. Each sample was tested in parallel five times.

3 RESULTS

3.1 Basis of the heat treatment process

The TG curves of SCG in different atmospheres show in Figure 1. The mass loss of the two atmospheres is roughly the same at 310 °C. There have 5% of the mass loss in the first stage occurred at 200 °C, probably due to the volatilization of free and bound water (Zarrinbakhsh et al., 2016). The most significant mass loss begins at 240 . It is caused by the breakdown of small molecular weight substances and hemicellulose. After 310 , ASCG is oxidized and decomposed. To avoid excessive weight loss of SCG, a heat treatment temperature of 240 degC was selected. Lignin and cellulose decompose at lower temperatures.

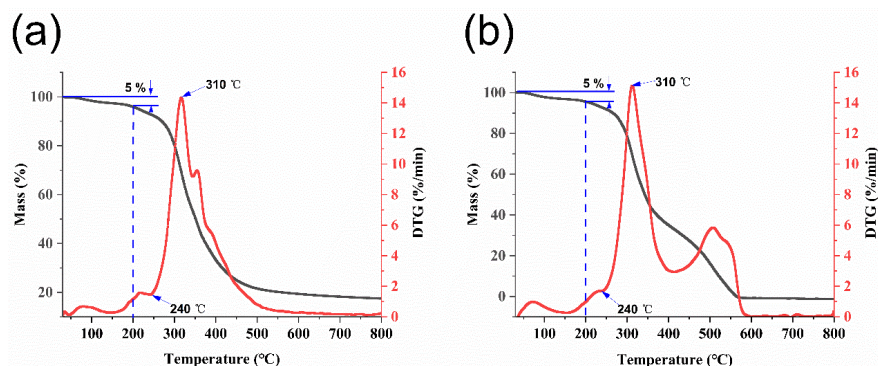


FIGURE 1 The TG curves of SCG under (a) N2 and (b) air atmosphere

3.2 Characterization of SCG

The influence of the heat treatment atmosphere on the color and microstructure of SCG was investigated. The digital images of SCG, NSCG, and ASCG are shown in Figure 2 (a-c). The colors of the SCG, NSCG, and ASCG are light brown, dark brown, and light black, respectively. The blackening degree of the ASCG is darker than that of the NSCG. The color shifts indicate that SCG will be carbonized to some degree at the same temperature, regardless of the atmosphere. In addition, the SEM images corresponding to the three samples are shown in Figure 2 (d-f). It can be found that they are agglomerate. But after heat treatment, the surface of particles becomes fluffy and the adhesion degree of particles decreases markedly. It is the result of partial volatilization of small molecular weight materials and low molecular weight hemicellulose (van der Stelt et al., 2011).

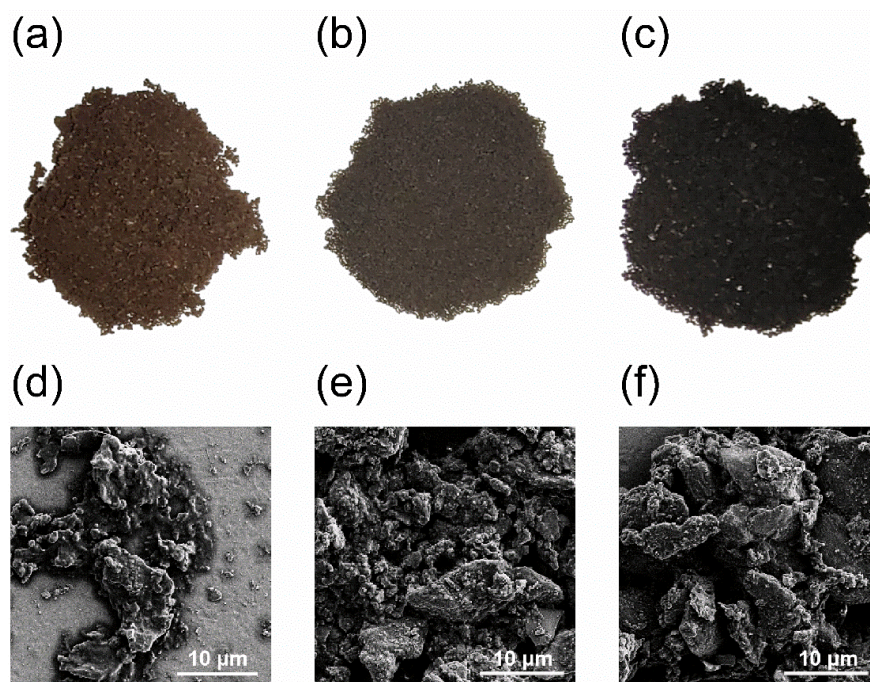


FIGURE 2 The digital images of (a) SCG, (b)NSCG , and (c) ASCG; The SEM images of (d) SCG,(e) NSCG, and (f) ASCG

Through the microscope, we observed the SCG under different atmospheres and statistically analyzed its particle size distribution, as shown in Figure 3. Figure 3 (a-c) shows that the original SCG is brown, and the color after heat treatment in different atmospheres is black. This is the same as the color reflected in the digital camera. Figure 3 (d-f) corresponds to the particle size distribution of SCG, NSCG , and ASCG, respectively. From the distribution map, the particle size of the three SCG showed a normal distribution, and the average particle size of the SCG was 0.204 mm, while the average particle size of the SCG after heat treatment in different atmospheres decreased to 0.188 and 0.186, respectively. The decrease of particle size indicates that heat treatment can effectively improve the grindability of SCG under the same grinding time, especially in air atmosphere.

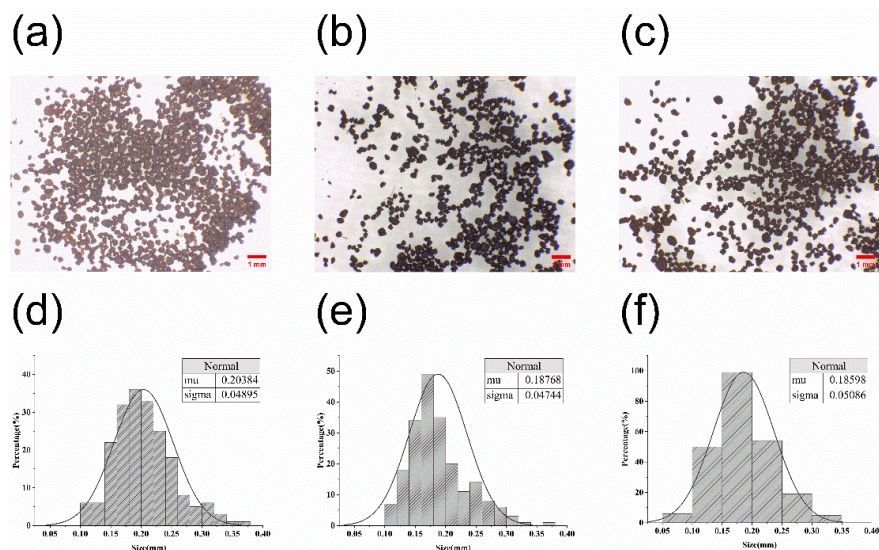


FIGURE 3 The microscope images of (a) SCG, (b) NSCG, and (c) ASCG; The distribution map of (d) SCG, (e) NSCG, and (f) ASCG

To observe the influence of the atmosphere on the functional groups in SCG, we obtained the FTIR spectra of SCG samples, as shown in Figure 4 (a). $3600-3100\text{ cm}^{-1}$ is ascribed to the vibration peak of the O-H group. $3000-2700\text{ cm}^{-1}$ is attributed to the tensile vibration region of C-H. The range of oxygen-containing functional groups is between 1800 and 900 cm^{-1} , such as carbonyl group, carboxyl group, an ether bond, etc. (Silverstein and Bassler, 1962). The effect of heat treatment on the functional groups of SCG is insignificant. However, the peak intensity of ASCG diminished significantly, because heat treatment reduced the content of O-H groups and other oxygen-containing functional groups (Hussin et al., 2018).

The bar chart of SCG residual oil content and SCG relative weight loss rate is shown in Figure 4 (b). The residual oil content of the SCG used in this experiment is about 14%, and that of NSCG is about 13%, with little change, but the ASCG is close to 10%. The results showed that air atmosphere heat treatment was more beneficial to the oxidative decomposition of oil in SCG. In terms of relative weight loss, ASCG is twice that of NSCG. The cause is the evaporation of oil and other ingredients.

The results of the water contact angle of the three SCG samples are shown in Figure 4 (c). The water contact angle of SCG is 93.86° , indicating that SCG showed weak hydrophobicity. The water contact angles of NSCG and ASCG are 100.39° and 103.44° , respectively. The hydrophobicity of SCG is enhanced, especially ASCG. The O/C ratio of SCG decreased, resulting in enhanced hydrophobicity (van der Stelt et al., 2011).

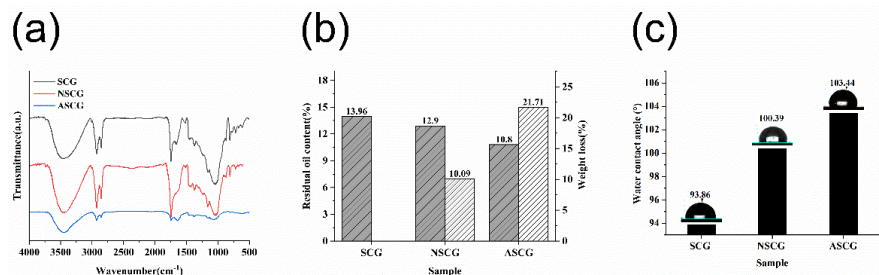


FIGURE 4 (a) FTIR spectra, (b) Residual oil content and weight loss of different SCG, (c) Water contact angle of SCG samples

Through the characterization of SCG, a series of data show that atmosphere has a certain influence on SCG. The most important performance is the residual oil content, which affects the diversity and comminution of SCG. In addition, hydrophobicity also changed significantly. Then we explore the effect of SCG, NSCG, and ASCG as fillers on PP performance.

3.3 Characterization of SCG/PP composites

3.3.1 Dispersion of SCG in PP matrix and Mechanical properties

The dispersion of SCG, NSCG, and ASCG in PP was observed by microscope and the mechanical properties of the samples are shown in Figure 5. As can be seen from the picture, SCG (a) has a large agglomeration and uneven distribution in PP, and the dispersion of NSCG (b) has not been significantly improved. However, ASCG (c) aggregates in PP became smaller and dispersed evenly. Combined with the character analysis of SCG, this observation can be attributed to the fact that the residual oil content of SCG and NSCG is greater than that of ASCG. The presence of oil causes agglomeration and affects the dispersity of SCG.

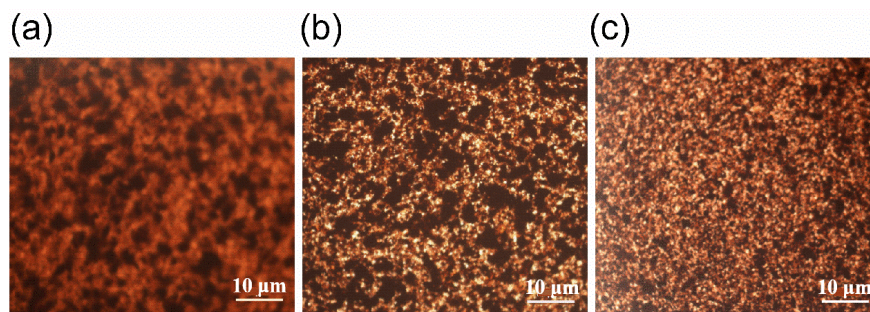


FIGURE 5 Microscope images of composites: (a) SCG/PP, (b) NSCG/PP, and (c) ASCG/PP

3.3.2 Water contact angle and Water absorption of SCG/PP composites

The water contact angle is one of the methods to characterize the hydrophilicity of materials. Figure 6 (a) is the result of the water contact angle. It shows the contact angle of PP is 84.37° , exhibiting weak hydrophilicity. The contact angle of the SCG/PP composite is 79.7° , which is smaller than that of PP. The water contact angle of NSCG/PP and ASCG/PP composites are 84.14° and 87.31° , respectively, which is close to or greater than that of PP. The contact angle of SCG/PP is more hydrophilic. It may be due to the poor dispersion of SCG in PP, resulting in high surface roughness and surface energy of the material, so the water wettability is stronger. After heat treatment, the dispersion of SCG in PP is uniform, the interface compatibility is better, and the relative probability of defects is small.

The water absorption capacity of plastic is closely related to its service life, so we test the water absorption rate of the samples, as shown in Figure 6 (b). It is worth noting that SCG/PP has the highest water absorption rate of 1.41%, followed by NSCG/PP with 1.2%, and ASCG/PP has the lowest water absorption rate of 0.9%. The hydrophobicity of the filler itself will affect the water absorption of the composite. With the addition of filler, the water absorption of the composites increased significantly. In addition, the water absorption for composites is closely related to the interfacial gap and defect. The material with better interface compatibility has less water absorption. The above data prove that SCG with air atmosphere heat treatment is more advantageous as a filler in solving the problem of interface compatibility. Food packaging materials should have good ability to block water. The stronger the hydrophobicity and the weaker the water absorption capacity, the more valuable it is in the preparation of finished products.

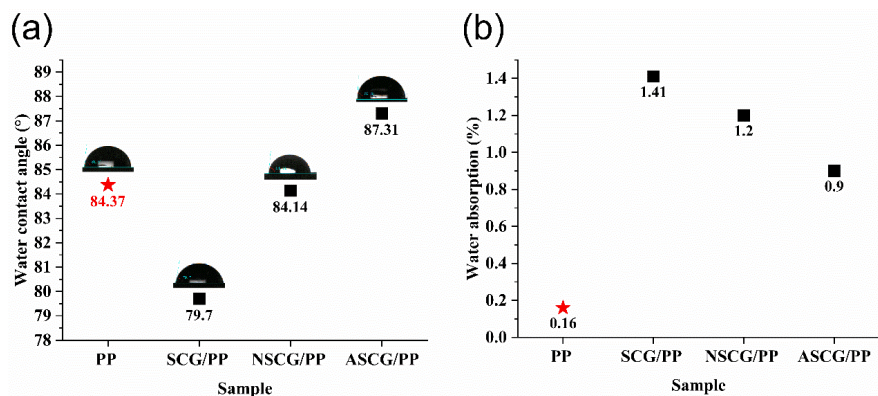


FIGURE 6 (a) Water contact angle, (b) Water absorption of PP and SCG/PP composites

3.3.3 Thermal stability

To study the influence of SCG under different heat treatment conditions on the thermal stability of PP composite, the thermal decomposition curve of the composite was tested, as shown in Figure 7. The initial thermal decomposition temperature of PP is 385 °C. After adding filler, the thermal stability of PP decreases, which is manifested as the advance of the initial thermal decomposition temperature. The thermal decomposition trend was similar after the addition of fillers, and the first stage of thermal decomposition was attributed to the partial decomposition of SCG. Compared with the SCG/PP composite, the thermal stability of the NSCG/PP and ASCG/PP composite are slightly improved, and the initial thermal decomposition temperature is increased from 265 to 280 . After heat treatment, the O/C ratio of SCG decreases and has stronger thermal stability (Leow et al., 2021). However, the thermal stability of SCG/PP composites treated in different atmospheres is similar, indicating that SCG fillers treated in different atmospheres have little effect on the thermal stability of PP. The results of the specific thermogravimetric values are summarized in Table 1.

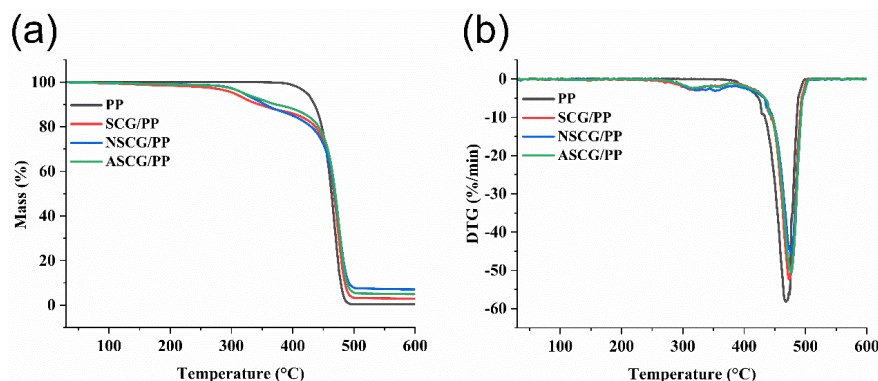


FIGURE 7 (a) TG, (b) DTG curve of PP and SCG/PP composites

TABLE 1 Mass loss temperature of PP and SCG/PP composites

Sample	Initial mass loss /	Maximum mass loss /	Final mass loss /
PP	385	468	500
SCG/PP	265	473	505
NSCG/PP	280	476	505
ASCG/PP	280	476	505

3.3.4 DSC

The melt-crystallization behavior of the polymer is determined by DSC. Figure 8 is represented the DSC curves of PP and SCG/PP composites. It can be seen from the melting curve (a) that the melting peak moves to low temperatures at different degrees, which is the result of the dilution effect caused by the addition of filler. In addition, the crystallinity of PP decreased after the addition of SCG, because the regularity of PP molecular chain was destroyed by the addition of filler SCG. In addition, the cross-linking effect between the two restricts the movement of polymer molecular chain, and the crystal growth of PP is restricted, thus reducing the crystallization ability. The crystallization curve (b) shows all the crystallization peaks are single exothermic peaks, indicating that SCG does not affect the crystal type of PP. During the cooling process, the crystallization peak moved slightly to a high temperature after the addition of SCG, and the degree of undercooling decreased, indicating that SCG played a role in promoting heterogeneous nucleation and making PP crystallize at a higher temperature. Table 2 is the data table of DSC test results.

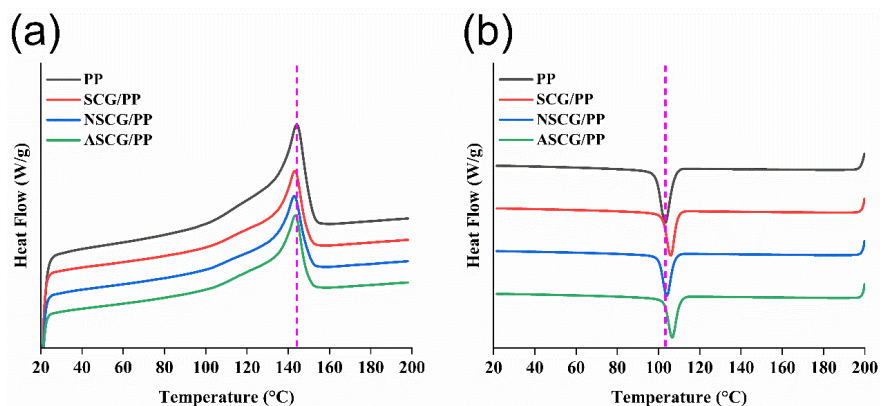


FIGURE 8 The DSC curves of PP and SCG/PP composites

TABLE 2. DSC results of pure PP and SCG/PP composites

Sample	$T_m /$	$\Delta H_m / J \cdot g^{-1}$	$T_c /$	$\Delta H_c / J \cdot g^{-1}$	$\Delta T /$	$X_c / \%$
PP	144.2	130.6	103.5	109.7	40.7	62.49
SCG/PP	143.2	109.6	105.9	92.2	37.3	52.44
NSCG/PP	143	110.2	104	91.1	39	52.73
ASCG/PP	143.5	107.9	106.6	89.2	36.9	51.63

3.3.5 Mechanical properties

The mechanical properties of the samples are shown in Figure 9. Figure 9 (a) is the tensile strength of the sample. The tensile strength of the composites are lower than that of pure PP. Compared with PP, the tensile strength of SCG/PP and NSCG/PP composites decreased by 56.3 % and 53.3 %, respectively, while ASCG/PP only decreased by 34.4 %. As shown in Figure 9 (b), the elongation at break decreased by 61.9 %, 67.2 % and 43.8 %, respectively. In addition, the elastic modulus of the composite increases, as shown in Figure 9 (c). The larger the elastic modulus, the harder the material. SCG acts as an inactive filler, which causes force concentration inside pp, resulting in a decrease in the tensile strength of pp. The different dispersion degree of the three fillers in PP leads to the difference of mechanical properties. In contrast, ASCG / PP is stronger and tougher. This can meet the most basic anti-cracking requirements for food packaging materials.

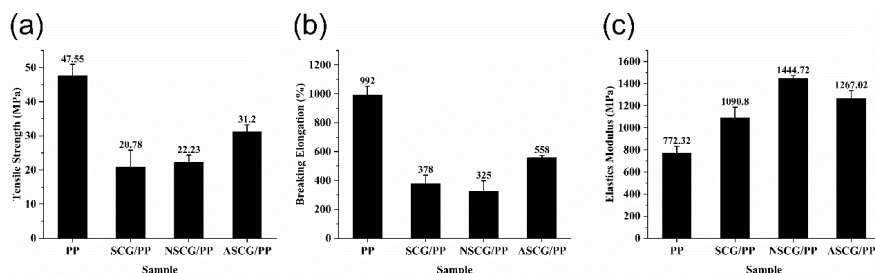


FIGURE 9 The mechanical properties of PP and SCG/PP composites

4 CONCLUSION

In summary, SCG was successfully used as a filler for PP to produce biomass-plastic composites. The coffee oil in SCG is removed more efficiently under air atmosphere than under nitrogen atmosphere at the same temperature. The obtained SCG holds a better affinity with PP by increasing the hydrophobicity, which further improves the water absorption, hydrophobicity, and mechanical properties of the resulting SCG/PP composite. The job offers a simple method for the preparation of biomass-plastic composites at a relatively low cost and an eco-friendly process. The composite shows potential applications in the field of food packaging.

Acknowledgement

This research work was financially supported by bilateral joint R&D project of Zhejiang Province (2022C04027).

CONFLICT OF INTEREST STATEMENT

The authors declare that they have no known competing financial interests or personal relationships that could have appeared to influence the work reported in this paper.

DATA AVAILABILITY STATEMENT

All data generated or analyzed during this study are included in this published article.

ORCID: Yurong Cai.

<http://orcid.org/0000-0003-1942-8931>

REFERENCES

- Arya, S.S., Venkatram, R., More, P.R., Vijayan, P., 2022. The wastes of coffee bean processing for utilization in food: a review. *J. Food Sci. Technol.* 59, 429–444. <https://doi.org/10.1007/s13197-021-05032-5>
- Ballesteros, L.F., Teixeira, J.A., Mussatto, S.I., 2014. Chemical, Functional, and Structural Properties of Spent Coffee Grounds and Coffee Silverskin. *Food Bioprocess Technol.* 7, 3493–3503. <https://doi.org/10.1007/s11947-014-1349-z>
- Bensalah, H., Raji, M., Abdellaoui, H., Essabir, H., Bouhfid, R., Qaiss, A. el kacem, 2021. Thermo-mechanical properties of low-cost “green” phenolic resin composites reinforced with surface modified coir fiber. *Int. J. Adv. Manuf. Technol.* 112, 1917–1930. <https://doi.org/10.1007/s00170-020-06535-9>
- Bomfim, A., Oliveira, D., Voorwald, H., Benini, K., Dumont, M.-J., Rodrigue, D., 2022. Valorization of Spent Coffee Grounds as Precursors for Biopolymers and Composite Production. *Polymers* 14, 437. <https://doi.org/10.3390/polym14030437>
- Branca, C., Di Blasi, C., Elefante, R., 2006. Devolatilization of Conventional Pyrolysis Oils Generated from Biomass and Cellulose. *Energy Fuels* 20, 2253–2261. <https://doi.org/10.1021/ef0601059>

- Branca, C., Di Blasi, C., Russo, C., 2005. Devolatilization in the temperature range 300–600K of liquids derived from wood pyrolysis and gasification. *Fuel* 84, 37–45. <https://doi.org/10.1016/j.fuel.2004.07.007>
- de Almeida-Couto, J.M.F., Abrantes, K.K.B., Stevanato, N., Silva, W.R. da, Wisniewski Jr, A., da Silva, C., Cabral, V.F., Cardozo-Filho, L., 2022. Oil recovery from defective coffee beans using pressurized fluid extraction followed by pyrolysis of the residual biomass: Sustainable process with zero waste. *J. Supercrit. Fluids* 180, 105432. <https://doi.org/10.1016/j.supflu.2021.105432>
- Franca, A.S., Oliveira, L.S., 2019. Chapter 17 - Coffee, in: Pan, Z., Zhang, R., Zicari, S. (Eds.), *Integrated Processing Technologies for Food and Agricultural By-Products*. Academic Press, pp. 413–438. <https://doi.org/10.1016/B978-0-12-814138-0.00017-4>
- Frias, J.P.G.L., Nash, R., 2019. Microplastics: Finding a consensus on the definition. *Mar. Pollut. Bull.* 138, 145–147. <https://doi.org/10.1016/j.marpolbul.2018.11.022>
- Hussin, H.W., Abdan, K., Salit, M.S., Bakar, E.S., 2018. Physical changes and FTIR analysis of kenaf core fiber heat treated in air. *IOP Conf. Ser. Mater. Sci. Eng.* 368, 012036. <https://doi.org/10.1088/1757-899X/368/1/012036>
- Jamari, S.S., Vennu, S.V., Ghazali, S., Abd Rahim, S., 2021. Effect of spent coffee grounds and rice husk amount towards the swelling properties of hydrogel using graft polymerization. *Mater. Today Proc.* 41, 140–143. <https://doi.org/10.1016/j.matpr.2020.12.1200>
- Kalebek, N.A., 2021. Fastness and antibacterial properties of polypropylene surgical face masks dyed with coffee grounds. *J. Text. Inst.* 1–7. <https://doi.org/10.1080/00405000.2021.1926129>
- Koh, E., Hong, K.H., 2019. Preparation and properties of wool fabrics dyed with spent coffee ground extract. *Text. Res. J.* 89, 13–19. <https://doi.org/10.1177/0040517517736469>
- Kumar, R., Strezov, V., Weldekidan, H., He, J., Singh, S., Kan, T., Dastjerdi, B., 2020. Lignocellulose biomass pyrolysis for bio-oil production: A review of biomass pre-treatment methods for production of drop-in fuels. *Renew. Sustain. Energy Rev.* 123, 109763. <https://doi.org/10.1016/j.rser.2020.109763>
- Le, B.A., Okitsu, K., Imamura, K., Takenaka, N., Maeda, Y., 2020. Ultrasound Assisted Cascade Extraction of Oil, Vitamin E, and Saccharides from Roselle (*Hibiscus Sabdariffa* L.) Seeds. *Anal. Sci.* 36, 1091–1097. <https://doi.org/10.2116/analsci.20p073>
- Leow, Y., Yew, P.Y.M., Chee, P.L., Loh, X.J., Kai, D., 2021. Recycling of spent coffee grounds for useful extracts and green composites. *RSC Adv.* 11, 2682–2692. <https://doi.org/10.1039/D0RA09379C>
- Madyaratri, E.W., Ridho, M.R., Aristri, M.A., Lubis, M.A.R., Iswanto, A.H., Nawawi, D.S., Antov, P., Kristak, L., Majlingová, A., Fatriasari, W., 2022. Recent Advances in the Development of Fire-Resistant Biocomposites—A Review. *Polymers* 14, 362. <https://doi.org/10.3390/polym14030362>
- McNutt, J., He, Q. (Sophia), 2019. Spent coffee grounds: A review on current utilization. *J. Ind. Eng. Chem.* 71, 78–88. <https://doi.org/10.1016/j.jiec.2018.11.054>
- Moustafa, H., Guizani, C., Dupont, C., Martin, V., Jeguirim, M., Dufresne, A., 2017. Utilization of Torrefied Coffee Grounds as Reinforcing Agent To Produce High-Quality Biodegradable PBAT Composites for Food Packaging Applications. *ACS Sustain. Chem. Eng.* 5, 1906–1916. <https://doi.org/10.1021/acssuschemeng.6b02633>
- Mueanmas, C., Nikhom, R., Petchkaew, A., Iewkittayakorn, J., Prasertsit, K., 2019. Extraction and esterification of waste coffee grounds oil as non-edible feedstock for biodiesel production. *Renew. Energy* 133, 1414–1425. <https://doi.org/10.1016/j.renene.2018.08.102>
- Nurman, S., Yulia, R., Irmayanti, I., Noor, E., Candra Sunarti, T., 2021. Optimizing Anti-inflammatory Activities of Arabica Coffee Ground (*Coffea arabica* L.) Nanoparticle Gel. *Jundishapur J. Nat. Pharm. Prod.* 16. <https://doi.org/10.5812/jjnpp.102673>

- Parra-Campos, A., Eduardo Ordonez-Santos, L., 2019. Natural pigment extraction optimization from coffee exocarp and its use as a natural dye in French meringue. *Food Chem.* 285, 59–66. <https://doi.org/10.1016/j.foodchem.2019.01.158>
- Qasim, U., Ali, M., Ali, T., Iqbal, R., Jamil, F., 2020. Biomass derived Fibers as a Substitute to Synthetic Fibers in Polymer Composites. *ChemBioEng Rev.* 7, 193–215. <https://doi.org/10.1002/cben.202000002>
- Ragauskaitė, D., Šlinkšienė, R., 2022. Influence of Urea on Organic Bulk Fertilizer of Spent Coffee Grounds and Green Algae *Chlorella* sp. *Biomass. Sustainability* 14, 1261. <https://doi.org/10.3390/su14031261>
- Rodrigues, M.O., Abrantes, N., Gonçalves, F.J.M., Nogueira, H., Marques, J.C., Gonçalves, A.M.M., 2018. Spatial and temporal distribution of microplastics in water and sediments of a freshwater system (Antuã River, Portugal). *Sci. Total Environ.* 633, 1549–1559. <https://doi.org/10.1016/j.scitotenv.2018.03.233>
- Santhanarajan, A.-E., Han, Y.-H., Koh, S.-C., 2021. The Efficacy of Functional Composts Manufactured Using Spent Coffee Ground, Rice Bran, Biochar, and Functional Microorganisms. *Appl. Sci.* 11, 7703. <https://doi.org/10.3390/app11167703>
- Silverstein, R.M., Bassler, G.C., 1962. Spectrometric identification of organic compounds. *J. Chem. Educ.* 39, 546. <https://doi.org/10.1021/ed039p546>
- Unugul, T., Kutluk, T., Gürkaya Kutluk, B., Kapucu, N., 2020. Environmentally friendly processes from coffee wastes to trimethylolpropane esters to be considered biolubricants. *J. Air Waste Manag. Assoc.* 1995 70, 1198–1215. <https://doi.org/10.1080/10962247.2020.1788664>
- van der Stelt, M.J.C., Gerhauser, H., Kiel, J.H.A., Ptasinski, K.J., 2011. Biomass upgrading by torrefaction for the production of biofuels: A review. *Biomass Bioenergy* 35, 3748–3762. <https://doi.org/10.1016/j.biombioe.2011.06.023>
- Watteau, F., Dignac, M.-F., Bouchard, A., Revallier, A., Houot, S., 2018. Microplastic Detection in Soil Amended With Municipal Solid Waste Composts as Revealed by Transmission Electronic Microscopy and Pyrolysis/GC/MS. *Front. Sustain. Food Syst.* 2, 81. <https://doi.org/10.3389/fsufs.2018.00081>
- Wu, H., Hu, W., Zhang, Y., Huang, L., Zhang, J., Tan, S., Cai, X., Liao, X., 2016. Effect of oil extraction on properties of spent coffee ground–plastic composites. *J. Mater. Sci.* 51, 10205–10214. <https://doi.org/10.1007/s10853-016-0248-2>
- Zarrinbakhsh, N., Wang, T., Rodriguez-Uribe, A., Misra, M., Mohanty, A.K., 2016. Characterization of Wastes and Coproducts from the Coffee Industry for Composite Material Production. *BioResources* 11, 7637–7653. <https://doi.org/10.15376/biores.11.3.7637-7653>
- Zhang, S., Yang, X., Gertsen, H., Peters, P., Salánki, T., Geissen, V., 2018. A simple method for the extraction and identification of light density microplastics from soil. *Sci. Total Environ.* 616–617, 1056–1065. <https://doi.org/10.1016/j.scitotenv.2017.10.213>
- Zhang, Y., Kang, S., Allen, S., Allen, D., Gao, T., Sillanpää, M., 2020. Atmospheric microplastics: A review on current status and perspectives. *Earth-Sci. Rev.* 203, 103118. <https://doi.org/10.1016/j.earscirev.2020.103118>